Article

US oil and gas system emissions from nearly one million aerial site measurements

https://doi.org/10.1038/s41586-024-07117-5

Received: 22 December 2022

Accepted: 23 January 2024

Published online: 13 March 2024

Check for updates

As airborne methane surveys of oil and gas systems continue to discover large emissions that are missing from official estimates[1–4], the true scope of methane emissions from energy production has yet to be quantified. We integrate approximately one million aerial site measurements into regional emissions inventories for six regions in the USA, comprising 52% of onshore oil and 29% of gas production over 15 aerial campaigns. We construct complete emissions distributions for each, employing empirically grounded simulations to estimate small emissions. Total estimated emissions range from 0.75% (95% confidence interval (CI) 0.65%, 0.84%) of covered natural gas production in a high-productivity, gas-rich region to 9.63% (95% CI 9.04%, 10.39%) in a rapidly expanding, oil-focused region. The six-region weighted average is 2.95% (95% CI 2.79%, 3.14%), or roughly three times the national government inventory estimate[5]. Only 0.05–1.66% of well sites contribute the majority (50–79%) of well site emissions in 11 out of 15 surveys. Ancillary midstream facilities, including pipelines, contribute 18–57% of estimated regional emissions, similarly concentrated in a small number of point sources. Together, the emissions quantified here represent an annual loss of roughly US$1 billion in commercial gas value and a US$9.3 billion annual social cost[6]. Repeated, comprehensive, regional remote-sensing surveys offer a path to detect these low-frequency, high-consequence emissions for rapid mitigation, incorporation into official emissions inventories and a clear-eyed assessment of the most effective emission-finding technologies for a given region.

Reduction in methane emissions from oil and gas systems is important in regard to climate change mitigation (https://www.globalmethanepledge.org/). However, technology limitations have hampered efforts to determine these emissions accurately on regional or national scales, with studies often producing divergent estimates[7–11]. Here we show that comprehensive aerial surveys, measuring most assets and hydrocarbon production in a region, can reliably estimate regional emissions by source. We integrate approximately one million aerial site measurements into emissions inventories for six regions in the USA, comprising 52% of onshore oil and 29% of gas production, over 15 aerial campaigns (https://www.enverus.com/solutions/energy-analytics/ep/). We construct emissions distributions by employing empirically grounded simulations to estimate small emissions. Total estimated emissions range from 0.75% (95% CI 0.65%, 0.84%) of covered natural gas production in a high-productivity, gas-rich region to 9.63% (95% CI 9.04%, 10.39%) in an expanding, oil-focused region. The six-region weighted average is roughly three times the national government inventory estimate[5]. Only 0.05–1.66% of well sites contribute the majority (50–79%) of well site emissions in 11 out of 15 surveys. A small fraction of ancillary midstream facilities contribute 18–57% of estimated regional emissions. The emissions quantified represent about US$1 billion annual loss in commercial gas value and US$9.3 billion in annual social cost[6]. Our approach offers a path for detection of low-frequency, high-consequence emissions for rapid mitigation, incorporation into official emissions inventories and assessment of effective emission-finding technologies for a given region.

Ensuring swift reductions in methane emissions from oil and natural gas systems requires an accurate understanding of total emissions in a region and how they are distributed. Such regional estimates help shape national policy priorities and track climate progress. A detailed understanding of the distribution of emissions, including the relative sizes of underlying facility-level emissions and the types of facilities that emit most, helps ensure prudent regional deployment of appropriate emission-sensing and -mitigation technologies.

Current US government emissions estimates are generally based on coarse emission factors, often relying on incomplete data[9,12]. This approach has been found to undercount emissions by up to 40%, as estimated by ground measurement studies at up to around 1,000 sites[11]. However, recent remote-sensing surveys conducted aerially and by satellite, covering tens or hundreds of thousands of sites, have discovered a substantial number of point-source methane emissions up to three orders of magnitude larger than those reported by the

[1]Department of Energy Science and Engineering, Stanford University, Stanford, CA, USA. [2]Kairos Aerospace, Sunnyvale, CA, USA. [3]Carbon Mapper, Pasadena, CA, USA. [4]Jet Propulsion Laboratory, California Institute of Technology, Pasadena, CA, USA. [5]Arizona Institutes for Resilience, University of Arizona, Tucson, AZ, USA. [6]Present address: Lawrence Berkeley National Laboratory, Berkeley, CA, USA. [7]Present address: Highwood Emissions Management, Calgary, Alberta, Canada. ✉e-mail: evansherwin@lbl.gov

aforementioned ground-based studies[1–4,13–17]. In at least some cases, these low-probability but high-consequence sources contribute most of the regional total[3,14].

Historically, no method existed to integrate aerial measurements of large emission sources with inventory-derived smaller sources, such as those in the US Greenhouse Gas Inventory (GHGI), to form a complete estimate of all emissions. In this paper we estimate emissions across six comprehensively measured major producing regions by merging the results of approximately one million site visits with an empirically grounded statistical model of smaller emission sources[7,11].

This approach leverages the ability of aerial surveys to rapidly screen vast areas for large emissions while simultaneously estimating emissions too small for detection by aerial technology. We also avoid double counting in cases in which simulated and aerially measured emissions distributions overlap. In the process we construct a complete distribution, from the smallest to the largest sources at the regional scale, leveraging comprehensive aerial surveys as well as a state-of-the-art, component-level emission simulation tool[18]. We define a comprehensive survey as including measurements of at least 50% of well sites and 80% of natural gas production in a region.

A previous study took steps in this direction, by combining aerial measurements with emissions simulation methods for 10% of well sites and 60% of midstream facilities in British Columbia, Canada[10]. Another recent study similarly estimated the emissions size distribution in the Permian, by joining comprehensive Carbon Mapper measurements with more sensitive aerial measurements at roughly 16% of well sites[19]. These studies advanced measurement-informed emissions estimation but require extrapolation to 84–90% of well sites and did not systematically measure pipeline infrastructure, as discussed in Supplementary Information 1.

Our method specifically facilitates evaluation of various use cases for the rapidly growing global fleet of commercial and government methane-sensing satellites and airborne systems[20–22]. Point-source methane detection satellite constellations, such as GHGSat and Carbon Mapper, could also comprehensively survey a selected region over time, generally with a lower level of detection sensitivity[21,23,24]. Furthermore, the distributions generated here can help assess multitiered methods of finding and mitigating methane emissions.

Combining measurements with simulations

We generate unified methane emissions distributions for surveyed oil and gas assets in six US oil- and gas-producing regions: the Permian, San Joaquin, Denver-Julesburg, Uinta and Fort Worth basins and Appalachian Pennsylvania (PA; Fig. 1a). Of the 15 aerial surveys, 11 are comprehensive, with the Pennsylvania and Permian 2020 and 2021 campaigns still covering at least 10% of well sites and 39% of natural gas production. These surveys include 986,238 well site measurements across all six regions, resulting from roughly 1,150 h of aerial data collection (detailed in Supplementary Information 2 and Supplementary Table 9). We define a measurement as an instance in which an aircraft flew over a well site or other facility and collected data. The surveys also include measurements of midstream infrastructure, including compressor stations, gas processing plants and pipelines. Note that, because of the comprehensive flight pattern used in these surveys, the average hour of data collection measures hundreds of sites, often simultaneously. The surveyed areas within these regions comprise 29% of onshore US gas production and 52% of oil production. We combine 15 large aerial surveys, conducted by Kairos Aerospace (Kairos) and researchers leading the Carbon Mapper project, with an empirically grounded emissions simulation method described previously[18]. We refine this model with input parameters based on regional characteristics and estimate small-source midstream emissions based on state-level and national GHGI data[5,14,18,25]. We demonstrate that our combined emissions distribution is consistent with major ground-based and aerial methane measurement studies, as shown in Supplementary Information 1.

For all oil- and gas-producing well sites covered in each surveyed region we first compute two site-level emissions inventories: one based on aerial measurements and the other using the emissions simulation tool described previously[18] to account for emissions we know are present but that aerial surveys probably would not see. We consider a well site to be a point location that may contain multiple wells and supplementary equipment such as liquids tanks, flares and separators. Figure 1c provides a high-level overview of the 1,000-realization Monte Carlo-based method we use to synthesize these two emissions inventories into a unified estimate of the distribution of methane emissions across surveyed well sites, which allows estimation of total emissions.

In its lower detection range an aerial system may detect smaller emissions only part of the time. This means that for every emission detected in this size range the survey may have missed other similar-sized emissions. For example, if the probability of detecting an emission of size x is one in three and one such emission is detected, this implies that two similar emissions were probably missed, tripling the estimated contribution of this detection to estimated campaign-wide emissions. For Kairos we use 234 controlled methane releases in the partial detection range to determine the probability of detecting emissions of varying size[14,20], described further in Supplementary Information 4.7. We do not have commensurate peer-reviewed controlled methane release data for the Carbon Mapper system, and correct for partial detection only in Kairos campaigns.

Aerial surveys also cover midstream assets such as gathering and transmission pipelines, compressor stations and gas processing plants, as shown in Fig. 1b. We estimate aerially measured and partially detected midstream emissions using the same approach as above. We do not have sufficient asset location data or emissions simulation tools for midstream infrastructure to estimate site-level emissions below the aerial detection limit. Instead we estimate these emissions based on the Environmental Protection Agency (EPA) national and state-level GHGI, removing the fraction of emissions underlying those estimates that would be detectable by Kairos or Carbon Mapper[5,25]. Because Kairos data used in this study are the product of proprietary commercial surveys, these data are fully anonymized and include no identifying information for covered operators or their assets (Supplementary Information 4).

Note that, in each Monte Carlo iteration for each of the 15 campaigns, we select only one emission value for each surveyed site, randomly choosing from all visits to that site, including those with and without aerial methane detections. Were we instead to treat each aerial site visit within a campaign as a completely independent measurement, this could introduce substantial bias if a subset of assets not representative of the full survey area is disproportionately oversampled, as demonstrated in Supplementary Information 5. Note that we do not estimate methane emissions from local distribution, oil refining and transportation, or from liquefied natural gas operations, that occur at facilities largely outside the surveyed regions. The resulting inventory is valid for the surveyed assets only at the time(s) of measurement and cannot necessarily be extrapolated to the full region over an extended time period—for example, annual emissions from a complete oil- and gas-producing basin—because the surveyed region may not be representative and emissions may change over time.

Estimated methane loss rates—the emitted fraction of methane produced from oil and natural gas activity in a given region—vary widely across the studied US regions. Estimated rates are as low as 1.08% (95% CI 0.98%, 1.18%) in the Denver-Julesburg basin in Colorado in 2021 and 0.75% (95% CI 0.65%, 0.84%) in a high-productivity area of the Pennsylvania portion of the Appalachian basin, as shown in Fig. 2. By contrast, for the New Mexico Permian 2018–2020 campaign the loss rate is 9.63% (95% CI 9.04%, 10.39%), one order of magnitude higher. The remaining campaigns range from roughly 2 to 6% methane loss

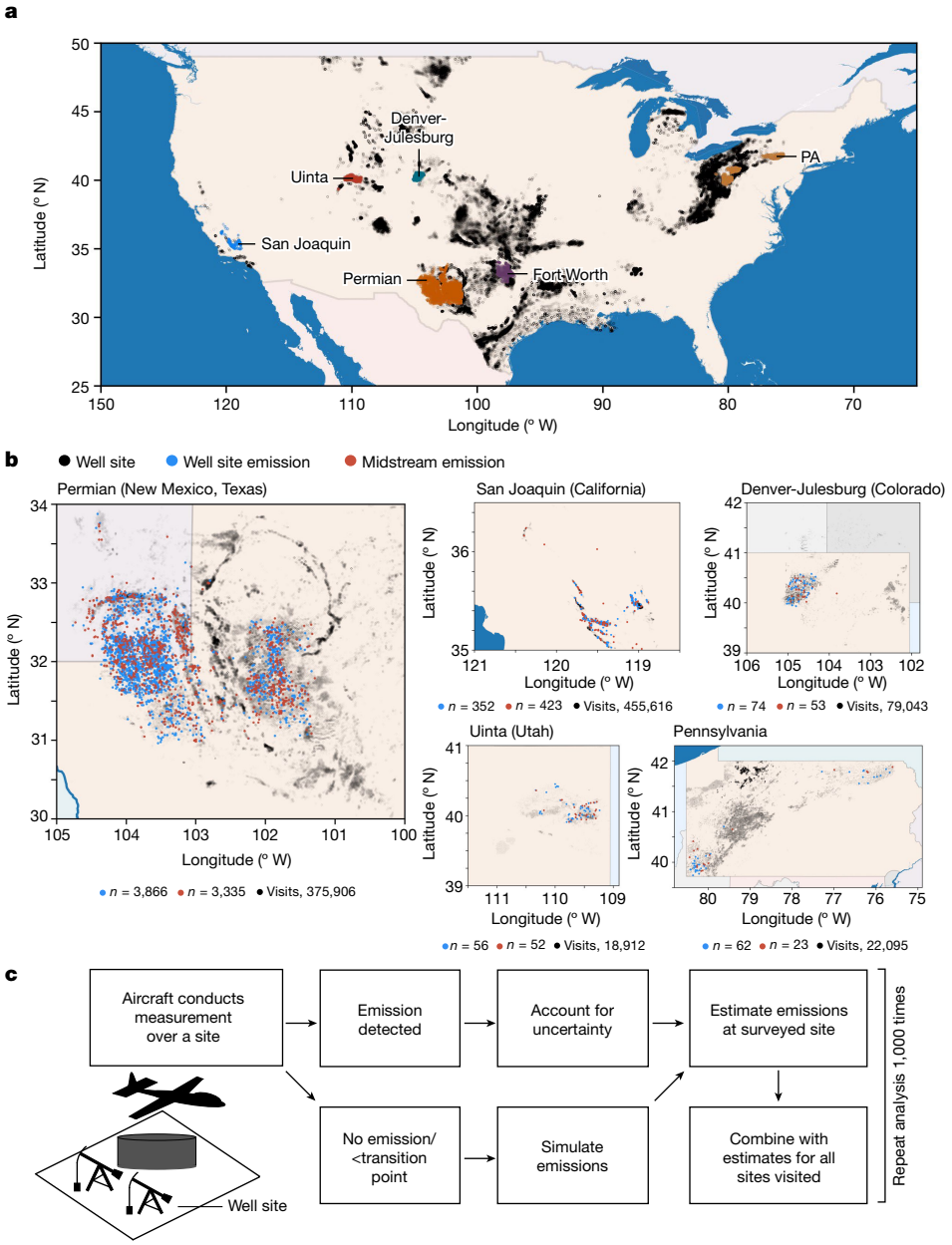

Fig. 1 | Survey maps and methods summary. a, Surveyed well sites. Remaining active US oil and gas wells coloured black. **b**, All aerially detected emissions from well sites (blue) and midstream infrastructure (red). Insets, visits denotes total count of well site visits (measurements) for each region, alongside counts of the number of emissions detected from well sites and midstream infrastructure. **c**, Site-level emissions estimation workflow. If emissions are detected during an aerial measurement at a well site, which may contain multiple wells and other equipment, or at a midstream asset, that emissions estimate is used directly after accounting for measurement uncertainty and partial detection probability (for smaller emissions that may not be detected by aerial systems in all instances). If no emission is detected at a well site, we estimate emissions using an emissions simulation tool described previously[18]. For midstream assets we use GHGI simulations to estimate aggregate regional midstream emissions below the aerial detection limit. We also use simulated emissions if an aerially measured emission is below the emission size at which simulated emissions dominate. To characterize uncertainty in total emissions in the surveyed region we repeat this stochastic process 1,000 times for each of the surveyed sites via Monte Carlo analysis, randomly drawing from all aerial measurements at each site with—and, for well sites—without aerially detected emissions. **a**,**b**, Note that Fort Worth coverage and emission data are not shown, to preserve anonymization. See Supplementary Information 3 for full map source information.

rates. The production-weighted loss rate across the most comprehensive campaign in each of the six regions is 2.95% (95% CI 2.79%, 3.14%), rising to 4.60% (95% CI 4.38%, 4.84%) when excluding the Pennsylvania campaign, which focuses on a high-productivity subregion. Note that the Pennsylvania and 2019 Carbon Mapper Permian campaigns have the highest natural gas production, equivalent to over 10,000 t CH_4 per hour each, as shown by the brown bars in Fig. 2. These loss rates and methane production levels assume a conservatively high methane fraction of 90% from ref. 11. If the actual methane fraction is lower, these loss rates would increase correspondingly, as discussed in Supplementary Information 6. These loss rates should not be used directly in life-cycle assessment without first accounting for the oil produced alongside natural gas, as discussed in Supplementary Information 7.

Most of these estimates are far larger than the national EPA GHGI, which places the 2020 US-wide onshore methane loss rate at 1.01% (95% CI 0.81%, 1.22%), after exclusion of municipal distribution systems,

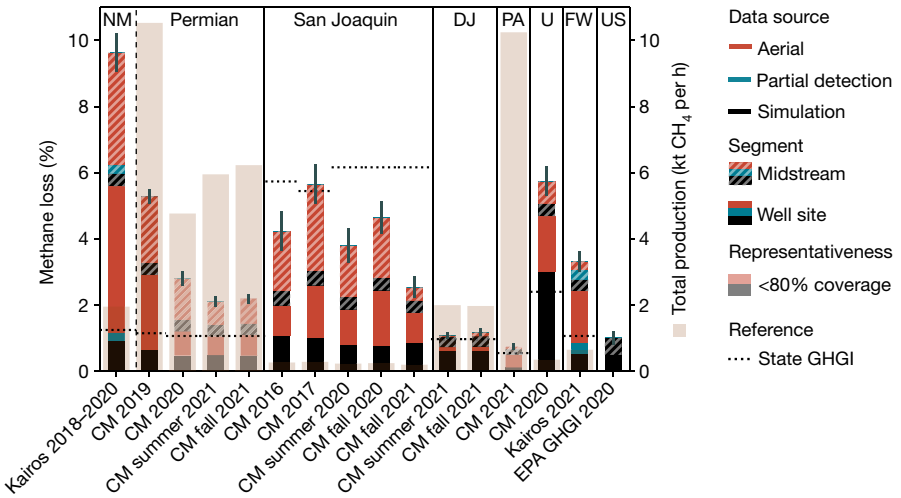

Fig. 2 | Estimated methane loss as a fraction of methane production. Data derived from oil and natural gas well sites and midstream assets (for example, pipelines and compressor stations) for all Kairos and Carbon Mapper (CM) campaigns in this study in the Permian, San Joaquin, Denver-Julesburg (DJ), Pennsylvania, Uinta (U) and Fort Worth (FW) regions. Colours represent aerially measured emissions (red), implied aerially detectable emissions in the partial detection range (teal, Kairos only) and estimated emissions from component-level simulation (black). Hatched bars represent midstream assets, and dashed lines are corresponding estimates from the EPA state-level GHGI, which form the basis for simulated midstream emissions estimates, with the 2020 national estimate for production and midstream shown in full on the right[5,25]. Brown semitransparent bars represent methane production in each region covered (right *y* axis) except for the whole USA (https://www.enverus.com/solutions/energy-analytics/ep/), assuming that natural gas is 90% methane[11]. The Kairos Permian campaign covers only the New Mexico Permian whereas Carbon Mapper extends into Texas. Whereas most campaigns cover over 80% of total gas production and at least 50% of regional well sites, semitransparent bars are focused disproportionately on high-production areas, which may not have the same emissions profile as the region as a whole. Error bars represent 95% CI, including multiple forms of uncertainty (Supplementary Information 4.2).

crude oil transportation and refining and post-meter emissions for consistency with this study[5]. These loss rates also generally exceed state-specific EPA inventories, shown as dashed lines in Fig. 2, although these estimates roughly align for the Denver-Julesburg and the studied region of Pennsylvania and the EPA value actually exceeds our estimate for four of the five San Joaquin campaigns[25] (see Supplementary Information 4 for further description of our treatment of EPA GHGI estimates).

Excluding airborne measurements and using only the full simulated distribution, regional emission rates for well sites align with EPA estimates to within plus or minus 50% for seven of the 15 campaigns. In the remaining eight campaigns simulated emissions reach a maximum of 68.0% higher than the GHGI in the Uinta and a minimum of 85.8% lower in the summer 2020 San Joaquin campaign (see Supplementary Information 2 and Supplementary Table 13 for further discussion of the reasons for these discrepancies).

Multiple surveys across the oil-focused San Joaquin basin demonstrate substantial variation in loss rate over time. The five San Joaquin campaigns find loss rates as low as 2.54% (95% CI 2.20%, 2.91%) in fall 2021, and as high as 5.64% (95% CI 5.04%, 6.34%) in 2017.

Even large surveys of the same region can produce divergent results if they cover different areas. Loss rates in the five Permian campaigns vary from 2.10% (95% CI 1.94%, 2.27%) in the fall 2021 campaign, focusing on high-productivity areas, to 9.63% (95% CI 9.04%, 10.39%) in the New Mexico Permian for 2018–2020. The largely overlapping 2019 survey of both Texas and New Mexico finds 5.29% (95% CI 5.08%, 5.53%; Supplementary Information 2 and 12).

This area-specific variation highlights the need to use comprehensive, or at least representative, aerial surveys when estimating regional emissions. For this reason Fig. 2 uses semitransparent bars to represent methane loss rate estimates from the Permian 2020 and 2021 campaigns, as well as from the Pennsylvania 2021 campaign, all of which disproportionately focus on high-productivity areas and cover less than 80% of natural gas production and less than 50% of well sites in the regions in question. For simulated well site emissions we account for the productivity of surveyed well sites, as described in Supplementary Information 4.4 and 14, but this simply improves the fidelity of simulated emissions within the region covered. As a result, our estimates from these less comprehensive campaigns are accurate for the high-productivity regions surveyed but are probably a conservatively low estimate of loss rates from the full region (for example, the entire Permian basin or all of Pennsylvania, respectively). Given the widely observed inverse relationship between the productivity of a well site and its rate of methane loss[26], these high-productivity surveys probably provide a lower bound on the corresponding regional methane loss rate. This is particularly the case in Pennsylvania, where site-level field measurements of low-producing wells suggest that our simulation may be systematically underestimating these emissions in this region (discussed further in Supplementary Information 1.2.2)[26].

In all cases midstream emissions are a substantial fraction of the total, representing 42–57% of total estimated oil and gas emissions in the Permian basin and falling as low as 18% in the Uinta. Supplementary Tables 10–15 provide additional summaries of regional emissions estimates.

Most emissions can often be detected aerially

Aerially measured emissions play a major role in nearly all basins, contributing 50–81% of the total in all 12 Permian, San Joaquin, Pennsylvania and Fort Worth campaigns. This rises as high as 84% in the New Mexico Permian after accounting for missed emissions in the partial detection range of the aerial system. The fraction of aerially measured emissions falls to 41% in the Uinta and to 14–20% in the Denver-Julesburg. Considering only emissions at well sites, aerially measured emissions contribute 50–79% of the total in 11 campaigns.

Many new methane-sensing technologies have emerged in the past few years. To assess the fraction of total emissions detected by technology with a given sensitivity in each region for a large campaign, Fig. 3 shows the full well site-level emissions distribution for all actively producing well sites covered in each of the 15 campaigns. Note that these

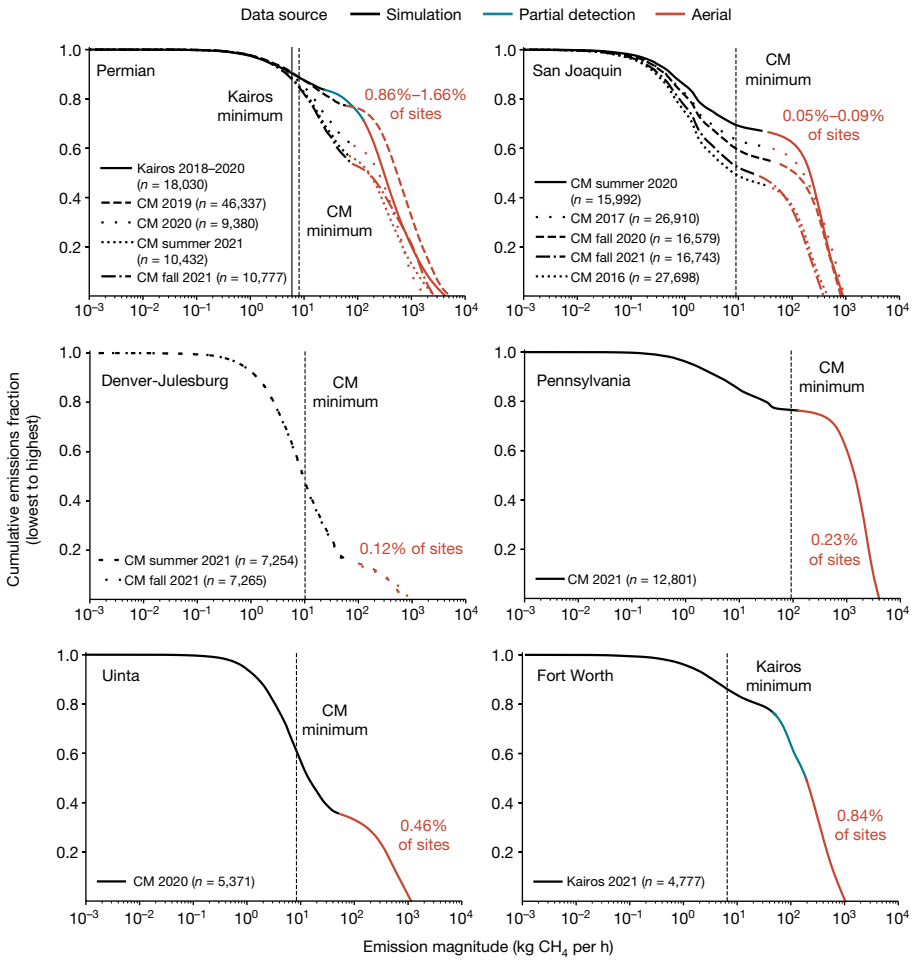

Fig. 3 | Cumulative well site methane emissions by region. The fraction of total emissions represented by well sites emitting at least a given amount of methane. Red represents direct measurements from aerial campaigns by Kairos and Carbon Mapper (CM), with the total number of well sites surveyed listed for each campaign in the legend and the fraction of sites with aerially detected emissions in the inset. Black represents simulated emissions at surveyed well sites with relatively low emissions. For Kairos campaigns, aerial emissions estimates include a correction for partial detection (teal) for smaller emissions based on single-blind controlled methane release testing. A similar correction for CM is not possible because commensurate blinded and peer-reviewed test data are not yet available. Vertical lines represent the minimum detected emission for each technology in a given region. The transition point away from simulated emissions represents the size beyond which aerially detected emissions consistently dominate simulated emissions.

distributions do not include midstream emissions, because we do not have site-level simulated emissions estimates in that case. Each point on these distributions represents a well site emission magnitude on the *x* axis, and the fraction of total estimated regional emissions coming from well sites emitting at least that amount on the *y* axis.

Despite their substantial contribution to the total in all cases, aerially detected emissions are present at only a small fraction of sites at any given time. In the Permian basin, an average of 0.86–1.66% of total well sites are emitting in a given Monte Carlo realization. This fraction falls to 0.05–0.09% of sites in the San Joaquin, with the remaining regions between the two. Furthermore, over 50% of well sites in the San Joaquin campaigns have zero simulated emissions. Thus, although previous literature focused on ground-based measurements found that 5% of measurements often contributed 50% of total emissions[27], this study finds that less than around 1% of measurements contribute over 50% of total emissions in 12 of 15 cases. The relatively infrequent occurrence of disproportionately contributing methane sources, consistent across study regions, supports the notion that both sensor sensitivity and scalability must be considered together when optimizing for a given methane detection technology in a given region[14]. See Supplementary Information 8, Supplementary Table 25 and Supplementary Figs. 13–18 for further discussion on the shape of the emissions distribution, which generally resembles a log-normal for simulated emissions and a power law for emissions measured aerially or by satellite.

The raw distributions of measured and simulated emissions often overlap for some ranges of emission size. To avoid double counting we designate a transition point between the measured and simulated distributions, defined as the site-level emission magnitude beyond which aerially measured emissions contribute more to the regional total than simulated emissions (Supplementary Information 4.8 and 9). As a result, some small emissions detected in most campaigns are not included in the combined distribution. This is likely because they fall within the partial detection range of the system, which can vary depending on the sensitivity of the sensor, flight altitude, automated and manual quality control processes and local environmental conditions including wind, sun angle, surface reflectance and vegetation cover. Whereas we correct for missed emissions in the partial detection range for Kairos surveys using the method described previously[14], commensurate single-blind, controlled-release testing data for Carbon Mapper are unavailable. In addition, Carbon Mapper conducted flights at different altitudes across campaigns, as described in Supplementary Information 2, affecting the lower detection range.

The absence of a correction in the partial detection range for Carbon Mapper campaigns, coupled with variation in detection capabilities

introduced by flight altitude and other above-mentioned factors, probably explains the somewhat higher transition points observed compared with Kairos campaigns. In the San Joaquin and Pennsylvania distributions, relatively flat areas indicate a gap between the largest simulated and smallest measured emissions, suggesting that our estimates of total emissions in these regions may be conservative, due in part to missing emissions in this middle size range that exist but that were not captured by our method. Carbon Mapper personnel believe that the gap for Pennsylvania is due in part to high vegetative cover. In probability density function form, shown in Supplementary Information 8, this gap between simulated and measured emissions appears as a local minimum in emission frequency, generally ranging between 10 and 100 kg h^{-1}, followed by a local maximum for aerially measured emissions. It is unclear whether the underlying distribution has a true local minimum in this size range in some regions or whether this is entirely an artefact introduced by sensor minimum capabilities.

In some cases, aerially detectable emissions substantially exceed the aerially measured portion of the combined distribution. The vertical lines in Fig. 3 represent the minimum emission detected by each aerial technology in each region. In some instances this is close to the transition point, as in the Kairos New Mexico Permian campaign, which has a minimum detected emission of 5.9 kg h^{-1} and a transition point of 24.4 kg h^{-1}. This indicates that, although aerially measured emissions contribute 81% of total emissions, Kairos-detectable emissions constitute 90%. The gap is larger for the Denver-Julesburg, where aerially measured emissions are 14% of the total and Carbon Mapper-detectable emissions are 45% of the total. Although some of these detectable emissions may lie within an aerial technology's partial detection range, this illustrates that the distributions given in this paper provide a conservative estimate of the fraction of emissions that these technologies will see when deployed in the field.

The surveyed regions in this study contribute an estimated 6.2 million t y^{-1} of methane emissions (extrapolated to an annual basis), equivalent to total carbon dioxide emissions from fossil fuel use in Mexico, using a 20-year global warming potential[28,29]. At US$3 per 1,000 standard cubic feet (about US¢1 kWh^{-1}), this amounts to U$1.08 billion (95% CI US$1.02 billion, US$1.14 billion) in market value. The environmental damage from these emissions is roughly ten times higher, at US$9.3 billion (95% CI US$8.8 billion, US$9.9 billion) assuming a US$1,500 t^{-1} social cost of methane[6] (discussed further in Supplementary Information 10). These emissions, and thus their associated costs, are roughly three times the level predicted by the US GHGI[5].

Reconciling past studies

Our study includes 986,238 well site measurements (aerial flights over individual well sites) and also captures substantial associated midstream infrastructure, representing a three-order-of-magnitude advance over the ground-based measurement literature[30]. The result is a transformed overall understanding of methane emissions from oil and natural gas systems that is simultaneously consistent with the bulk of the related peer-reviewed literature.

The primary reason we estimate higher emissions is that the vast spatial extent of our campaigns ensures we measure emissions at the small fraction of sites, 1.66% or less, responsible for the majority of total emissions in all but four of our 15 campaigns. This fraction falls to 0.05–0.09% of sites in the San Joaquin. Across all 15 campaigns, aerially measured emissions average 74% of total estimated production and midstream emissions, as shown in Supplementary Information 2 and Supplementary Table 15.

Our regional estimates align closely with the most recent aerial mass balance flights and in situ sensor tower-based inversion methods in the Uinta, Denver-Julesburg and northeast Pennsylvania, and in a high-productivity area of the Permian[31–36]. This suggests that, despite disagreement with other site-level emissions estimation methods, we are accurately estimating total emissions to within statistical error. Furthermore, our results align with the estimates described previously[3] for five of the six study regions after accounting for differences in treatment of intermittency, as shown in Supplementary Information 1.4 and Supplementary Table 2. Our results do suggest that some regional flux estimates based on data from the TROPOMI satellite are probably conservative[37,38]. We discuss these and related studies further in Supplementary Information 1.

In addition, our emissions simulation tool aligns to within statistical error with site-level measurements of marginally producing oil and natural gas well sites in ref. 26 in four of the five overlapping regions, discussed further in Supplementary Information 1.2.2, Supplementary Table 1 and Supplementary Figs. 1–5 (ref. 26). This suggests that our simulated estimates for Pennsylvania may be conservative.

In other words, our study largely explains numerous apparently divergent results in the literature. 'Top-down' regional flux estimates based on in situ measurements from aircraft or ground-mounted towers match our numbers to within statistical error. Previous 'bottom-up' methods, scaling up component-level (for example, GHGI) or vehicle-based site-level measurements (for example, ref. 11), tend to both undersample and underestimate the tiny fraction of sites responsible, in many cases for the majority of total emissions[5,11]. The key to bridging this gap is measurement of the vast majority of total sites and accurate estimation of the largest emissions, supplementing this with best-in-class simulated estimates of the smaller emissions, as we do in this paper.

Illuminating the full extent of undercounting that may be occurring in official inventory estimates across the entire USA and internationally will require additional comprehensive measurement campaigns. Given the regional variability in emission rates we show in this work, an accurate estimate of US emissions will require surveying a large fraction of the 48% of onshore oil and 71% of natural gas production not covered here. Correspondingly, the working assumption, until proven otherwise, should be that aerially detectable sources contribute substantially to overall emissions for all global oil- and natural gas-producing regions and that these emissions can be quantified through comprehensive measurement campaigns.

In addition, national methane emissions estimates reported to the United Nations are probably conservative in many cases because countries often rely on GHGI emission factors[12], as described in Supplementary Information 11.

Keeping methane promises

This study hints at substantial methane emissions reductions, achievable through highly targeted intervention approaches. This could be accomplished by focusing on the small fraction of sites that contribute a large proportion of overall emissions, and by modifying equipment or operations at those sites to reduce emissions. These sites can be effectively flagged across large geographic areas by aircraft or dedicated satellites, such as those characterized in ref. 23. Future emissions modelling to assess the efficacy of such rapid screening methods in the six regions characterized here should use the distributions presented in this paper, or similar methods, at least for those campaigns with comprehensive spatial coverage. Furthermore, updated distributions can be fed into existing, peer-reviewed numerical models to generate more accurate estimates of field emissions and assess basin-specific efficacy of different leak detection and repair technologies and deployment strategies[39,40]. It should be stressed that achieving climate goals will also require substantial cuts in emissions below the detection limits of the aerial technologies used in this study.

Tracking of progress requires repeated surveys at regular intervals. Aerial surveys present a unique opportunity for comprehensive, periodic measurement with reliable quantification and the ability to detect the majority of total emissions volume in many regions. The

appropriate survey frequency will depend on the particular application. The US EPA draft methane rule for oil and gas well sites suggests monthly or bimonthly aerial survey frequency depending on instrument sensitivity[41]. Empirically validated regional area flux estimates—for example, relying on data from TROPOMI or MethaneSAT—can also help track regional emissions over time[21].

As demonstrated here, the generation of accurate emissions inventories will require fusing of datasets collected across scales. This becomes more important with the near-term deployment of a substantial fleet of dedicated point-source methane satellites, as well as the continued growth of commercial and public airborne data providers. Soon, measurement at a meaningful sensitivity may be possible anywhere on Earth. This will represent an enormous advance for understanding emissions in every hydrocarbon-producing country, with methane emissions detected at unprecedented accuracy, speed and scale. The method introduced in this study forms the basis for combining measurements at multiple scales to produce usable emissions inventories that will enable reliable, timely tracking of the rapid, unambiguous reductions in global methane emissions to which so many countries have committed.

Online content

Any methods, additional references, Nature Portfolio reporting summaries, source data, extended data, supplementary information, acknowledgements, peer review information; details of author contributions and competing interests; and statements of data and code availability are available at https://doi.org/10.1038/s41586-024-07117-5.

1. Duren, R. M. et al. California's methane super-emitters. *Nature* **575**, 180–184 (2019).
2. Cusworth, D. H. et al. Intermittency of large methane emitters in the Permian Basin. *Environ. Sci. Technol. Lett.* **8**, 567–573 (2021).
3. Cusworth, D. H. et al. Strong methane point sources contribute a disproportionate fraction of total emissions across multiple basins in the United States. *Proc. Natl Acad. Sci. USA* **119**, e2202338119 (2022).
4. Frankenberg, C. et al. Airborne methane remote measurements reveal heavy-tail flux distribution in Four Corners region. *Proc. Natl Acad. Sci. USA* **113**, 9734–9739 (2016).
5. US Environmental Protection Agency. *Inventory of U.S. Greenhouse Gas Emissions and Sinks: 1990–2020;* www.epa.gov/ghgemissions/inventory-us-greenhouse-gas-emissions-and-sinks-1990-2020 (2022).
6. Yarmuth, J. A. Inflation Reduction Act of 2022, H.R.5376, Public Law No. 117–169, https://www.congress.gov/bill/117th-congress/house-bill/5376/text (2022).
7. Brandt, A. R. et al. Methane leaks from North American natural gas systems. *Science* **343**, 733–735 (2014).
8. Conrad, B. M., Tyner, D. R., Li, H. Z., Xie, D. & Johnson, M. R. A measurement-based upstream oil and gas methane inventory for Alberta, Canada reveals higher emissions and different sources than official estimates. *Commun. Earth Environ.* **4**, 416 (2023).
9. US Environmental Protection Agency. *Methodology Report: Inventory of U.S. Greenhouse Gas Emissions and Sinks by State: 1990–2020;* https://www.epa.gov/ghgemissions/methodology-report-inventory-us-greenhouse-gas-emissions-and-sinks-state-1990-2020 (2023).
10. Johnson, M. R., Conrad, B. M. & Tyner, D. R. Creating measurement-based oil and gas sector methane inventories using source-resolved aerial surveys. *Commun. Earth Environ.* **4**, 139 (2023).
11. Alvarez, R. A. et al. Assessment of methane emissions from the U.S. oil and gas supply chain. *Science* **361**, 186–188 (2018).
12. Carras, J. N. et al. in *2006 IPCC Guidelines for National Greenhouse Gas Inventories* Ch. 4 (2006).
13. Irakulis-Loitxate, I. et al. Satellite-based survey of extreme methane emissions in the Permian basin. *Sci. Adv.* **7**, eabf4507 (2021).
14. Chen, Y. et al. Quantifying regional methane emissions in the New Mexico Permian Basin with a comprehensive aerial survey. *Environ. Sci. Technol.* **56**, 4317–4323 (2022).
15. Varon, D. J. et al. Satellite discovery of anomalously large methane point sources from oil/gas production. *Geophys. Res. Lett.* **46**, 13507–13516 (2019).
16. Varon, D. J. et al. High-frequency monitoring of anomalous methane point sources with multispectral Sentinel-2 satellite observations. *Atmos. Meas. Tech.* **14**, 2771–2785 (2021).
17. Lauvaux, T. et al. Global assessment of oil and gas methane ultra-emitters. *Science* **375**, 557–561 (2022).
18. Rutherford, J. S. et al. Closing the methane gap in US oil and natural gas production emissions inventories. *Nat. Commun.* **12**, 4715 (2021).
19. Kunkel, W. M. et al. Extension of methane emission rate distribution for Permian Basin oil and gas production infrastructure by aerial LiDAR. *Environ. Sci. Technol.* **57**, 12234–12241 (2023).
20. Sherwin, E. D., Chen, Y., Ravikumar, A. P. & Brandt, A. R. Single-blind test of airplane-based hyperspectral methane detection via controlled releases. *Elementa (Wash. D. C.)* **9**, 00063 (2021).
21. Jacob, D. J. et al. Quantifying methane emissions from the global scale down to point sources using satellite observations of atmospheric methane. *Atmos. Chem. Phys.* **22**, 9617–9646 (2022).
22. Bell, C. et al. Single-blind determination of methane detection limits and quantification accuracy using aircraft-based LiDAR. *Elementa (Wash. D. C.)* **10**, 00080 (2022).
23. Sherwin, E. D. et al. Single-blind validation of space-based point-source detection and quantification of onshore methane emissions. *Sci. Rep.* **13**, 3836 (2023).
24. Sherwin, E. D. et al. Single-blind test of nine methane-sensing satellite systems from three continents. *Atmospheric Meas. Tech.* **70**, 765–782 (2024).
25. US Environmental Protection Agency. *State GHG Emissions and Removals;* www.epa.gov/ghgemissions/state-ghg-emissions-and-removals (2022).
26. Omara, M. et al. Methane emissions from US low production oil and natural gas well sites. *Nat. Commun.* **13**, 2085 (2022).
27. Brandt, A. R., Heath, G. A. & Cooley, D. Methane leaks from natural gas systems follow extreme distributions. *Environ. Sci. Technol.* **50**, 12512–12520 (2016).
28. Crippa, M. et al. *Fossil CO_2 and GHG emissions of all world countries: 2019 report* (Publications Office of the European Union, 2019).
29. Masson-Delmotte, V. et al. (eds.) *Climate Change 2021: The Physical Science Basis. Contribution of Working Group I to the Sixth Assessment Report of the Intergovernmental Panel on Climate Change* (Cambridge Univ. Press, 2021).
30. Omara, M. et al. Methane emissions from natural gas production sites in the United States: data synthesis and national estimate. *Environ. Sci. Technol.* **52**, 12915–12925 (2018).
31. Peischl, J. et al. Quantifying atmospheric methane emissions from the Haynesville, Fayetteville, and northeastern Marcellus shale gas production regions. *J. Geophys. Res. Atmos.* **120**, 2119–2139 (2015).
32. Pétron, G. et al. A new look at methane and nonmethane hydrocarbon emissions from oil and natural gas operations in the Colorado Denver-Julesburg Basin: hydrocarbon emissions in oil & gas basin. *J. Geophys. Res. Atmos.* **119**, 6836–6852 (2014).
33. Barkley, Z. R. et al. Quantifying methane emissions from natural gas production in north-eastern Pennsylvania. *Atmos. Chem. Phys.* **17**, 13941–13966 (2017).
34. Peischl, J. et al. Quantifying methane and ethane emissions to the atmosphere from central and western U.S. oil and natural gas production regions. *J. Geophys. Res. Atmos.* **123**, 7725–7740 (2018).
35. Fried, A. & Dickerson, R. *Interim Report on Proposal Activities and No-Cost Extension Request: Continuous Airborne Measurements and Analysis of Oil & Natural Gas Emissions During the 2021 Denver-Julesburg Basin Studies.* Prepared for the Colorado Oil and Gas Conservation Commission and the Colorado Air Pollution Control; https://apcd.state.co.us/aqidev/tech_doc_repository.aspx?action=open%26file=CU_UMD_2021_Final_Report.pdf (2022).
36. Lin, J. C. et al. Declining methane emissions and steady, high leakage rates observed over multiple years in a western US oil/gas production basin. *Sci. Rep.* **11**, 22291 (2021).
37. Zhang, Y. et al. Quantifying methane emissions from the largest oil-producing basin in the United States from space. *Sci. Adv.* **6**, eaaz5120 (2020).
38. Schneising, O. et al. Remote sensing of methane leakage from natural gas and petroleum systems revisited. *Atmos. Chem. Phys.* **20**, 9169–9182 (2020).
39. Fox, T. A., Gao, M., Barchyn, T. E., Jamin, Y. L. & Hugenholtz, C. H. An agent-based model for estimating emissions reduction equivalence among leak detection and repair programs. *J. Clean. Prod.* **282**, 125237 (2021).
40. Kemp, C. E. & Ravikumar, A. P. New technologies can cost effectively reduce oil and gas methane emissions, but policies will require careful design to establish mitigation equivalence. *Environ. Sci. Technol.* **55**, 9140–9149 (2021).
41. US Environmental Protection Agency. *Standards of Performance for New, Reconstructed, and Modified Sources and Emissions Guidelines for Existing Sources: Oil and Natural Gas Sector Climate Review;* https://www.federalregister.gov/documents/2021/11/15/2021-24202/standards-of-performance-for-new-reconstructed-and-modified-sources-and-emissions-guidelines-for (2022).

Methods

We estimate the full distribution of the magnitude of well site methane emissions for 15 large-scale aerial surveys of at least 10% of well sites and at least 35% of natural gas production in each of six US regions. This includes campaigns by Kairos in the New Mexico Permian basin and the Fort Worth basin in Texas (focusing on the Barnett shale), alongside campaigns conducted by the Carbon Mapper-led team (including scientists from Jet Propulsion Laboratory (JPL), the University of Arizona and Arizona State University) in the Permian basin in New Mexico and Texas (four campaigns), California's San Joaquin basin (five campaigns), the Denver-Julesburg basin (two campaigns) as well as the Uinta basin and a high-productivity portion of the Appalachian basin in Pennsylvania (one campaign each)[1,2,42,43]. For midstream we show distributions of aerially measured emissions in Supplementary Information 9 and estimate emissions too small for reliable aerial detection based on the GHGI[5,25].

All campaigns use hyperspectral infrared spectroscopy to detect and quantify methane emissions using the spectral signature of methane in reflected sunlight. The quantification accuracy and minimum detection capabilities of the Kairos technology were independently validated in single-blind, controlled-release testing[20] (see ref. 44 for further detail surrounding the technology). The Carbon Mapper campaigns were conducted with the Airborne Visible-Infrared Imaging Spectrometer – Next Generation (AVIRIS–NG) spectrometer on a JPL-contract King Air B200 aircraft and an identical very-short-wavelength infrared imaging spectrometer on the Global Airborne Observatory (GAO) operated by Arizona State University, both described in ref. 2. The AVIRIS–NG and GAO systems have also undergone non-blinded, controlled-release testing for assessment of minimum detection limits and quantification accuracy[45], and single-blind testing of the quantification accuracy of the GAO system is currently under peer review[46].

Both teams use data from imaging spectrometers to estimate methane flux rates based on measured atmospheric methane enhancements retrieved from spectral radiances, combined with estimates of 10 m wind speeds from reanalysis products. For Kairos we combine reported wind-normalized emission rates with National Oceanic and Atmospheric Administration High-Resolution Rapid Refresh hourly instantaneous wind speed estimates for the New Mexico Permian survey[14], and using Dark Sky 1 min gust wind speed data for the Fort Worth survey (the two wind reanalysis products have a similar error profile[20]). Carbon Mapper uses the average High-Resolution Rapid Refresh wind speed estimate from the nearest nine reported grid values, averaged over the hour before, hour after and hour of a given measurement[1].

Kairos flights were conducted at roughly 900 m above ground level, and Carbon Mapper flights range from 3,000 to 8,500 m (described in detail in Supplementary Table 4). Both systems estimate methane enhancements based on the relative prevalence of certain frequencies of infrared light compared with other frequencies in reflected sunlight, described further in refs. 47,48. Supplementary Information 4.1 provides further discussion of uncertainty in these estimates; Supplementary Tables 2–9 and 24 and Supplementary Figs. 6–9 include additional summary statistics and figures describing the surveys.

Below we describe the steps taken to construct a complete emissions distribution from a comprehensive aerial measurement campaign through our quantitative approach, which we term the regional oil and gas aerial methane synthesis model.

Step 1: conduct a comprehensive aerial measurement campaign

To produce an aerial measurement-based regional emissions inventory for oil and natural gas production and midstream activity, one must first conduct a comprehensive aerial survey of the region in question. In this study we term a survey 'comprehensive' if it covers at least 50% of all active oil and natural gas well sites and at least 80% of natural gas production in the region in question, generally an oil- and natural gas-producing basin. Whereas future studies may use alternative definitions of comprehensive, it is noteworthy that measurement campaigns focusing only on high- or low-productivity areas of a region can produce misleading estimates of the overall regional methane loss rate, as illustrated in Supplementary Information 12 and Supplementary Fig. 19. Supplementary Tables 3 and 5 show coverage information for each survey in this study.

Step 2: estimate regional aerially measured emissions using Monte Carlo analysis

We first estimate the distribution of measured emissions in each aerially surveyed region as a function of emission size, using each emission source as the unit of analysis. Each oil or natural gas well site is a potential emission source. In midstream, facilities such as compressor stations and gas processing plants are potential emission sources, as are pipelines. For pipelines, each detected emission location is considered an emission source.

In many instances an emission source was surveyed multiple times, with emissions detected during only a fraction of aerial measurements. To account for this we apply Monte Carlo simulation to characterize the emission profile of the surveyed region. We simulate emissions from each emission source with at least one detected emission, drawing randomly from all aerial measurements at that location, including those with no detected emissions. We then randomly insert simulated error into each quantified emission based on estimates of quantification uncertainty, discussed further in Supplementary Information 4.1. We repeat this stochastic process for 1,000 Monte Carlo realizations to capture uncertainty. This method yields an unbiased estimate of total well site emissions in the surveyed region, as described in ref. 14. By analogous logic, it also yields an unbiased estimate of the size distribution of aerially visible emissions from the surveyed assets at the time(s) of measurement, but not the variance of total emissions (Supplementary Information 2.2 and Supplementary Fig. 10). The resulting emissions inventory covers only aerially detected emissions, treating emissions as zero at all sites at which emissions were not detected.

In the Kairos Fort Worth survey, 8.5% of detected emission plumes extended beyond the spectrometer's field of view and were thus classified as 'cutoff' and not quantified. We estimate emission magnitude for these emissions by drawing randomly from the distribution of quantified emissions for well sites and midstream infrastructure, respectively. The number of emission source measurements is not reported for ten of 11 pipeline emission sources in the Kairos Fort Worth survey, out of 72 identified emission sources. We assume these emissions are fully persistent, setting the number of measurements equal to the number of detected emissions at that source.

Note that campaigns in the same region with comparable well site coverage may cover different amounts of midstream infrastructure, which may affect estimated midstream emissions estimates. We do not have sufficient midstream asset location data to quantify this effect here. Supplementary Information 2 provides coverage information for each campaign.

Step 3: account for partial detection

For emissions approaching the minimum detection level of an aerial detection system, there may be a fractional probability of detection. If an aerial survey of a population of assets detects an emission of a size that corresponds to a known probability of detection of one in three, this implies that the survey probably missed two emissions of similar size. Thus, an aerial survey will tend to underestimate emissions in this partial detection range by a predictable amount.

We correct for this effect in the Kairos surveys in the New Mexico Permian and Fort Worth basins using probability of detection curves based on controlled-release testing[14,20] (Supplementary Information 4 and 4.7 and Supplementary Fig. 12).

Note that, for the Kairos campaigns, the partial detection correction accounts for less than 3% of total estimated emissions in the New Mexico Permian and less than 10% in Fort Worth. This suggests that the partial detection correction is not a major source of upward bias in our emissions estimates.

Carbon Mapper has conducted internal controlled-release testing to characterize its minimum detection range[45]. However, we do not have sufficient single-blind, controlled-release data to apply a similar correction to Carbon Mapper surveys, many of which were also conducted at varying altitude, further changing lower detection characteristics. This introduces conservatism into estimates of aerially measured emissions from Carbon Mapper campaigns.

Step 4a: simulate well site emissions

We then produce a comprehensive well site-level emissions inventory for the surveyed region as the basis for estimation of emissions missed by the aerial survey. An equally valid interpretation of our method is that we begin with a simulated emissions inventory and update that using observational data from an aerial survey. We simulate emissions at all surveyed well sites using a basin-scale emissions simulation tool[18]. The bottom-up emissions simulation begins with field measurements of the prevalence and magnitude of emissions at the component level—for example, valves, flanges and open-ended lines. It then converts these into probabilistic equipment-level emission factors based on component counts for different types of equipment—for example, separators, meters and wellheads.

We update this simulation tool with basin-specific equipment activity data from the EPA's Greenhouse Gas Reporting Program—for example, the number of wellheads and pneumatic controllers per site in a given productivity range, as well as production data, for probabilistic estimation of emissions at each well site in a given basin. Supplementary Tables 17–20 and Supplementary Fig. 11 provide summaries of relevant input data, and Supplementary Table 26 and Supplementary Figs. 20–25 include a summary of simulation results. This analysis thus estimates well site-level emission rates for all surveyed active oil and gas well sites in the six basins.

Simulated well site emissions are based on component-level measurements of methane emission frequency and magnitude, combined with counts of the number of each relevant component (for example, valves, connectors and open-ended lines) per piece of well site equipment (as listed in the previous paragraph). Equations (1) and (2) summarize the underlying mathematics behind this probabilistic emissions estimation method for a given basin, described in detail in Supplementary Information 4.4 and ref. 18.

$$Q_i = \Sigma_{j=1}^{n_{\text{equip}}} Q_{i,j} a_j \quad (1)$$

$$Q_{\text{basin}} = \Sigma_{i=1}^{n_{\text{wells}}} Q_i \quad (2)$$

where Q_i is simulated emissions for a given simulated well, i, and Q_{basin} is methane emissions from all wells across the oil- and gas-producing basin in question (accounting for associated wellpad equipment). The i index iterates across all wells in the basin, totalling n_{wells}. The j index iterates across equipment types, with a total of n_{equip} types. $Q_{i,j}$ is a randomly generated equipment-level emission factor for equipment type j at well i, drawing on empirical measurements of component counts per piece of equipment, the fraction of components emitting at a given time and component-level emission rates per emission, described further in ref. 18 and Supplementary Information 4.4; a_j is an equipment activity factor (equipment count per well) drawn from EPA GHGRP data for the basin containing the simulated region. Finally, wells are translated into well sites using the spatial clustering algorithm introduced in ref. 11. The result is a distribution of well site-level emissions based on Q_i values. Supplementary Information 13 shows simulated equipment-level emission factors across each study region.

We identify the number of wells surveyed in a given campaign by filtering the Enverus coordinates of all active wells in the relevant basin by each aerial survey area (https://www.enverus.com/solutions/energy-analytics/ep/). Enverus does not divide wells into well sites. We convert this count of wells to a count of well sites, assuming the average number of wells per site for the basin, derived from the 2020 basin-specific emissions simulation model results, which use the well-to-site clustering algorithm introduced in ref. 11. For the New Mexico Permian we rely on ref. 49 and for the San Joaquin 2016 and 2017 campaigns we rely on ref. 30, both of which apply a similar method (Supplementary Information 4.6).

To account for differences in well site productivity between the surveyed area and the basin as a whole, for each campaign we draw simulated emissions for each surveyed well site from an example with similar natural gas productivity. This ensures that simulated emissions are representative of the surveyed area but does not guarantee that the overall emissions estimate from the surveyed area will be representative of the basin as a whole, as illustrated in Supplementary Fig. 26 (Supplementary Information 4.5 and 14). Supplementary Tables 27–32 include productivity summary statistics by survey and basin. The result is simulated emission levels for all well sites covered by each aerial survey. Supplementary Table 16 gives additional details of uncertainty estimation in this approach.

Step 4b: Simulate midstream emissions

We do not have a site-level emissions simulation tool for midstream infrastructure that is comparable to the above well site emissions simulation method. Instead we rely on national and state-level GHGI estimates from EPA, which include reported annual values from 2016 to 2020 (refs. 5,25). These estimates are based on similar emissions simulation methods. We describe our approach in detail in Supplementary Information 4.9, and Supplementary Tables 22 and 23 provide additional summaries of our treatment of GHGI data.

Step 5a: combine aerially measured and simulated well site inventories

We then combine the generated well site-level inventories of aerially measured and simulated emissions from steps 2–4a. For each Monte Carlo realization we transition from simulated to measured emissions at the emission size at which measured emissions consistently dominate simulated emissions. This approach avoids double counting across aerial and simulated emissions inventories (Supplementary Information 4.8 and 9).

Note that this transition point may be larger than the smallest emission detected in the corresponding aerial survey; this is because aerial emissions detection systems generally detect only a particular fraction of emissions below a certain size. This partial detection range can vary depending on the technology, quality control processes and environmental conditions and thus raw aerial measurements may underestimate total emissions at the lower end of the detected range.

For Kairos we are able to correct the aerially measured emissions distribution for missed emissions in this partial detection range using results from single-blind, controlled-release testing[20] (Supplementary Information 4.7). Although Carbon Mapper has conducted some controlled-release testing to characterize minimum detection capabilities, we do not have sufficient data to apply similar correction factors, as discussed in Supplementary Information 4.1.

We therefore use measured emissions for all well sites with emissions larger than or equal to the transition point, after accounting for partial detection. We use simulated emissions for all other surveyed well sites.

Note that, if an aerial survey of a region detected no emissions, this method would simply reproduce the emissions simulation results with every surveyed site assigned comparatively small (sometimes zero)

simulated emission values, described further in Supplementary Information 8 and 13. This is because the method currently assumes that there is an emission size beyond which aerially measured emissions consistently dominate simulated emissions, which is the case in all campaigns in this study. As a result the emissions simulation forms a lower bound for our estimates, with aerially measured emissions only adding to (and not subtracting from) the simulated regional total. Future surveys with lower detection limits, alongside alternate methods of determining a transition point to allow for cases in which measured emissions in the full detection range are smaller than simulated emissions, should further reduce reliance on simulated emissions. See Supplementary Table 21 for the transition points computed for each survey.

Note that one could also employ a Bayesian approach to combining simulated and measured emissions distributions[50]. We do not do so here due to difficulties in combining nonparametric distributions in Bayesian updating, and because such Bayesian analysis would require subjective determination of the relative weight given to simulated and measured data.

Step 5b: combine aerially measured and simulated midstream inventories

Simulated midstream emissions inventories, derived from the EPA GHGI, are not disaggregated into site-level emissions. As a result we cannot directly apply the above method, removing all simulated emissions above (and all aerially measured emissions below) a transition point emission size.

Instead we remove a fraction of simulated midstream emissions corresponding to aerially visible emissions from key field measurements that underlie midstream emissions estimates from the GHGI, as described in Supplementary Information 4.9.

Step 6: estimation of methane fractional loss

We estimate campaign-specific fractional loss rate, L_c as follows:

$$L_c = \frac{E_c}{P_c} \quad (3)$$

where E_c is total estimated emissions from all well sites and midstream assets covered in the campaign, based on the combined distribution of aerially measured emissions, corrected for partial detection plus simulated emissions, as described in steps 1–5b. We then compute P_c, total methane production for all covered well sites, using the method described in Supplementary Information 4.5.

We then assume that this gas has a molar methane fraction of 90% in all basins[11], probably a conservatively high estimate more representative of transmission pipeline-ready natural gas than the gross gas production at the well site reported by Enverus (Supplementary Information 6). A lower molar methane fraction would reduce estimated methane production, thus increasing the estimated methane fractional loss rate.

Data availability

Anonymized emission and source data from the Kairos Fort Worth campaign are available at *Zenodo* https://doi.org/10.5281/zenodo.8302419 (ref. 51), from the Kairos Permian at *Zenodo* https://doi.org/10.5281/zenodo.10067753 (ref. 52). The remaining Kairos Aerospace data from this study are not available for open release due to confidentiality concerns. Kairos Aerospace is committed to working with research groups studying methane emissions. Access may be granted, but must be done directly through Kairos Aerospace. Interested researchers should contact research-collaborations@kairosaerospace.com. For sensitive Kairos and Enverus microdata, the published code contains aggregated summaries sufficient to reproduce key results in the paper: regional estimates of the magnitude and breakdown of methane emissions from oil and gas activity. In addition, our code repositories include all code used to aggregate these commercially sensitive microdata. All methane data from airborne campaigns led by the Carbon Mapper/JPL team since 2016 are available at https://doi.org/10.3334/ORNLDAAC/1727 and from refs. 1,2,42,43. Data required to reproduce maps of national and state boundaries within the USA are available at https://www.census.gov/geographies/mapping-files/time-series/geo/carto-boundary-file.html and from Esri, with national boundaries for Canada and Mexico at http://www.naturalearthdata.com/downloads/, lakes and rivers from the United States Geological Survey at https://www.sciencebase.gov/catalog/item/4fb55df0e4b04cb937751e02 and ocean boundaries from the Flanders Marine Institute at https://doi.org/10.14284/542. Source data are provided with this paper.

Code availability

The data and code required to reproduce the key results of this article, as well as 100,000 random samples from each simulated emissions distribution in this study, are available at *Zenodo* https://doi.org/10.5281/zenodo.10064774 (ref. 53) and https://doi.org/10.5281/zenodo.10073882 (ref. 54).

42. Cusworth, D. H. Methane plumes for NASA/JPL/UArizona/ASU Sep–Nov 2019 Permian campaign. *Zenodo* https://doi.org/10.5281/zenodo.5610307 (2021).
43. Cusworth, D. et al. Methane plumes from airborne surveys 2020–2021 (1.0). *Zenodo* https://doi.org/10.5281/zenodo.5606120 (2021).
44. Berman, E. S. F., Wetherley, E. B. & Jones, B. B. *Kairos Aerospace Technical White Paper: Methane Detection* (Version 1F); https://doi.org/10.17605/OSF.IO/HZG52 (2023).
45. Thorpe, A. K. et al. Mapping methane concentrations from a controlled release experiment using the next generation airborne visible/infrared imaging spectrometer (AVIRIS-NG). *Remote Sens. Environ.* **179**, 104–115 (2016).
46. El Abbadi, S. et al. Comprehensive evaluation of aircraft-based methane sensing for greenhouse gas mitigation. Preprint at eartharxiv.org/repository/view/5569/ (2023).
47. Branson, K., Jones, B. B. & Berman, E. S. F. *Kairos Aerospace Methane Emissions Quantification;* https://doi.org/10.17605/OSF.IO/2UNWQ (2021).
48. Thorpe, A. K., Frankenberg, C. & Roberts, D. A. Retrieval techniques for airborne imaging of methane concentrations using high spatial and moderate spectral resolution: application to AVIRIS. *Atmos. Meas. Tech.* **7**, 491–506 (2014).
49. Robertson, A. M. et al. New Mexico Permian Basin measured well pad methane emissions are a factor of 5–9 times higher than U.S. EPA estimates. *Environ. Sci. Technol.* **54**, 13926–13934 (2020).
50. Wasserman, L. *All of Statistics: A Concise Course in Statistical Inference* (Springer Science+Business Media, 2004).
51. KairosAerospace/stanford_fort_worth_data_2021: v1.0. *Zenodo* https://doi.org/10.5281/zenodo.8302419 (2023).
52. KairosAerospace/stanford_nm_data_2019: v1.0. *Zenodo* https://zenodo.org/records/10067753 (2023).
53. Sherwin, E. D. & Zhang, Z. Data and code for "US oil and gas system emissions from nearly one million aerial site measurements". *Zenodo* https://zenodo.org/records/10064774 (2023).
54. JSRuthe/BU_methane_model: Release for distributions paper. *Zenodo* https://zenodo.org/records/10073882 (2023).

Acknowledgements J. Kruguer of Kairos Aerospace provided data management support. T. Lauvaux, C. Giron and A. d'Aspremont provided satellite-derived data to support the analysis of power law behaviour. This work benefited from discussions with N. Boness, S. El Abbadi, B. Hmiel, E. Kort, G. Wayne, M. Omara, R. Gautam, D. Zavala-Araiza, S. Hamburg and R. Jackson. This study was funded by the Stanford Natural Gas Initiative, an industry consortium that supports independent research at Stanford University. Funding for AVIRIS–NG and GAO flight operations and/or data analysis referenced in this paper was provided by NASA's Carbon Monitoring System and Advanced Information System Technology programmes, as well as by Carbon Mapper, RMI the Environmental Defense Fund, the California Air Resources Board, the University of Arizona and the US Climate Alliance. Funding for Colorado overflights was provided by the Mark Martinez and Joey Irwin Memorial Public Projects Fund with the support of the Colorado Oil and Gas Conservation Commission and the Colorado Department of Public Health and Environment. Portions of this research were carried out at JPL, California Institute of Technology, under a contract with the National Aeronautics and Space Administration (no. 80NM0018D0004). GAO is managed by the Center for Global Discovery and Conservation Science at Arizona State University, and is made possible by support from private foundations, philanthropic individuals and Arizona State University.

Author contributions Conceptualization was the responsibility of E.D.S., A.R.B., E.S.F.B. and B.B.J. Resources were handled by A.R.B., E.S.F.B. and R.M.D. E.D.S., E.S.F.B., E.B.W., P.V.Y., D.H.C., Z.Z., J.S.R. and Y.C. undertook data curation. E.D.S., J.S.R., Z.Z. and Y.C. were responsible for software. Formal analysis was carried out by E.D.S., J.S.R. and Z.Z. A.R.B. supervised the project. Funding was acquired by A.R.B., E.S.F.B. and R.M.D. Investigation was carried out by E.D.S., E.S.F.B., E.B.W., D.H.C., A.K.T. and A.K.A. E.D.S. and Z.Z. undertook visualization. E.D.S.,

J.S.R., E.B.W. and P.V.Y. performed methodology. E.D.S. wrote the original draft. The project was administered by E.D.S. and A.R.B. All authors wrote, reviewed and edited the article.

Competing interests E.S.F.B., P.V.Y., B.B.J. and E.B.W. are employees of Kairos Aerospace. R.M.D., D.H.C. and A.K.A. are employees of the University of Arizona and seconded to the non-profit organization Carbon Mapper. The remaining authors declare no competing interests.

Additional information

Supplementary information The online version contains supplementary material available at https://doi.org/10.1038/s41586-024-07117-5.

Correspondence and requests for materials should be addressed to Evan D. Sherwin.

Peer review information *Nature* thanks Grant Allen and the other, anonymous, reviewer(s) for their contribution to the peer review of this work. Peer reviewer reports are available.